**Proceedings of the 28th IEEE**
**EMBS Annual International Conference**
**New York City, USA, Aug 30-Sept 3, 2006**



# Comparison of Current Densities measured in a Pig Heart during States of Ventricular Fibrillation and Post-mortem for different Defibrillation Electrode Positions

Tim P. DeMonte, *Member, IEEE,* Dawn B. Jorgenson, Dinghui Wang, Angela W. Ma, Adrian I. Nachman, and Michael L. G. Joy, *Member, IEEE*

***Abstract*—Current density imaging (CDI) is an MRI technique used to quantitatively measure current density vectors in biological tissue. A fast CDI sequence was developed that can image the whole body of a 4 kg pig in about 15 minutes. A state of ventricular fibrillation (VF) can be sustained for nearly 30 minutes allowing two complete CDI scans of the same subject. A single parameter, i.e. electrode position, is adjusted between the two scans for comparative analysis. This study compares the current density vector directions and current density magnitudes measured for two typical electrode positions, i.e. apex anterior (AA) and apex posterior (AP). The comparative experiment is repeated on the same subjects for states of immediate post-mortem and one hour post-mortem. Further, the acquired vector datasets are used to compute conductivity images of the heart.**

## I. Introduction

CURRENT density imaging (CDI) is an MRI technique that measures electrical current density magnitude and direction vectors in biological tissue where the currents are generated by an externally applied source synchronized with the MRI sequence [1]. A fast CDI technique based on a 3D fast gradient recalled echo (FGRE) MRI sequence was developed for imaging current densities associated with external defibrillation procedures [2]. This fast CDI sequence can scan 64 slices of vector data in about 15 minutes. Using a voxel size of 3.8 $mm^3$, the whole body of a 4 kg pig is covered by the scan. A state of ventricular fibrillation (VF) can be potentially sustained for up to 30 minutes, particularly in a smaller sized, i.e. 4 kg, animal. This time frame allows for two complete CDI datasets to be acquired during VF such that a single parameter of the experiment, i.e. electrode position, can be comparatively investigated. The experiments were repeated for states of immediate post-mortem (PM1) and about one hour post-mortem (PM2) to observe changes with tissue degradation.

The first step in data analysis is to isolate regions of interest by segmenting the anatomical MRI datasets. The regions of interest include the whole heart and subdivisions of the heart including ventricles, atria and aorta [3], [4]. For brevity, only the results pertaining to the whole heart are covered in this abstract.

Vector directions are analyzed in regions of interest using streamline analysis techniques [5]. A streamline representing the direction of current flow is computed by integrating the current density vectors along a curve $s$ which satisfies

$$ds = \left(\frac{dx}{J_x}\right) = \left(\frac{dy}{J_y}\right) = \left(\frac{dz}{J_z}\right), \quad (1)$$

where $J_x$, $J_y$ and $J_z$ are the three Cartesian components of the measured current density vectors.

Current density magnitude $|\mathbf{J}|$ is computed from the three measured components of current density as

$$|\mathbf{J}| = \sqrt{J_x^2 + J_y^2 + J_z^2} \quad (2)$$

Current density magnitude is computed throughout regions of interest and analyzed using statistical techniques such as mean and cumulative distribution.

Another useful method of analysis is computing the current flux through a region of interest [6]. The net flux is zero by definition; however, the flux entering (or exiting) a region gives a measure of how much current is reaching the region of interest. For flux computation, a surface is defined that passes halfway through the voxels located along the boundary of the region of interest. To avoid surface erosion, 2x1 derivative templates are used instead of the 3x3 Sobel templates [1], [7] typically used in CDI. Data shifting due to asymmetry of the template is corrected using linear interpolation to re-grid the data appropriately onto the surface.

Standard errors are computed for both the mean value of $|\mathbf{J}|$ and current flux. The standard error computations are based on standard deviations of the magnetic field

Manuscript received April 3, 2006. This work was supported in part by Philips Medical Systems (Seattle, USA defibrillation research group) and in part by MITACS Networks of Centres of Excellence (Canada).

T. P. DeMonte is with Field Metrica Inc., Toronto, ON M8V 1W1 Canada (phone: 416-259-9842; e-mail: tdemonte@fieldmetrica.com).

D. B. Jorgenson is with Philips Medical Systems, Seattle, WA 98121 USA (e-mail: dawn.jorgenson@philips.com).

D. Wang is with the Institute of Biomaterials and Biomedical Engineering, University of Toronto, Toronto, ON M5S 3G9 Canada (e-mail: dinghui.wang@utoronto.ca).

A. W. Ma is with the Institute of Biomaterials and Biomedical Engineering, University of Toronto, Toronto, ON M5S 3G9 Canada (e-mail: weijing.ma@utoronto.ca).

A. I. Nachman is with the Department of Mathematics and with the Department of Electrical and Computer Engineering, University of Toronto, Toronto, ON M5S 3G4 Canada (e-mail: adrian.nachman@utoronto.ca).

M. L. Joy is with the Institute of Biomaterials and Biomedical Engineering, University of Toronto, Toronto, ON M5S 3G9 Canada (e-mail: mikejoy@ecf.utoronto.ca).

**1-4244-0033-3/06/$20.00 ©2006 IEEE.**

measurements used to compose the current density vectors. The standard error in the average $|\mathbf{J}|$ was approximated as 1/3 the sum of the standard errors of the average $J_x$, $J_y$ and $J_z$. Further details of these standard error computations are beyond the scope of this abstract.

After acquiring two different current density vector sets, i.e. apex anterior (AA) and apex posterior (AP), for the same subject, it is possible to directly compute the relative isotropic conductivity image [8]. Suppose the two current density vector sets corresponding to AA and AP acquisitions are labeled $\mathbf{J}_1$ and $\mathbf{J}_2$, respectively. The gradient of the logarithm of the conductivity, $\sigma$, is computed as

$$\nabla \ln \sigma = \left(\frac{1}{M^2}\right)\{(\nabla \times \mathbf{J}_2 \cdot \mathbf{M})\mathbf{J}_1 - (\nabla \times \mathbf{J}_1 \cdot \mathbf{M})\mathbf{J}_2 + (\nabla \times \mathbf{J}_1 \cdot \mathbf{J}_2)\mathbf{M}\} \quad (3)$$

where $\mathbf{M} = \mathbf{J}_1 \times \mathbf{J}_2$. The conductivity can be obtained by integration of equation (3). This technique assumes the conductivity is isotropic.

## II. Methods

### A. Experimental Setup

The two electrode placements compared were apex anterior (AA) and apex posterior (AP). To facilitate quick switching between electrode placements, three flexible, pediatric, automatic external defibrillation (AED) electrodes were placed on the pig as shown in figs. 1(a) and 1(b).

### B. Experimental Procedure

Two experiments, i.e. #1 and #2, were performed on anesthetized landrace pigs weighing 4.0 kg and 4.6 kg, respectively. For each experiment, pavulon injections were used to minimize muscle contractions and VF was electrically induced via external defibrillation electrodes.

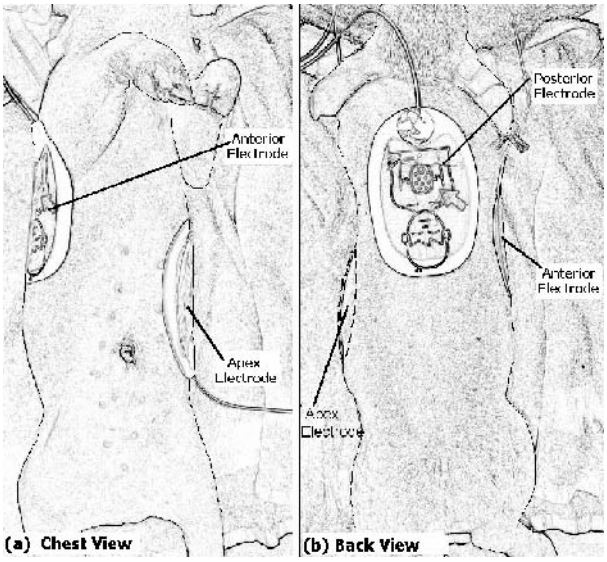


Fig. 1. Automatic External Defibrillation (AED) electrode positions on pig. Three electrodes were placed on pig in apex, anterior and posterior positions, as shown, to facilitate fast switching between electrode configurations. Chest view (a) and back view (b) of pig demonstrate the two electrode configurations of apex anterior (AA) and apex posterior (AP).

CDI commenced immediately after VF induction. MRI imaging parameters were 3.8 $mm^3$ voxels, 64 slices, 48 cm field of view, TR = TE = 10.0 ms and the MR receive coil was an MRI body coil. Current pulses applied to pigs were 4.7 ms x 58 mA for experiment #1 and 4.7 ms x 140 mA for experiment #2. The pigs were euthanized immediately after the VF scan and the experiment was repeated post-mortem (PM1) and once again (PM2).

### C. Analysis

MRI data was segmented to isolate the voxels corresponding to the heart. Streamline analysis of vector directions was applied to the whole body datasets. Current density magnitude, $|\mathbf{J}|$, was computed for voxels within the heart and statistical methods including mean value, standard error and cumulative distributions were applied to the data. Current flux and standard error were computed for voxels within the heart. Finally, the current density vector measurements for the two electrode positions were combined to compute relative conductivity images of the heart.

## III. Results

Vector directions are compared for AA and AP electrode positions and are shown in figs. 2 and 3. Figs. 2(a) and 2(b) show a chest view of the pig (experiment #1) during VF. The gray coloured portions of the image are a transparent iso-surface generated from the anatomical MRI datasets. This iso-surface indicates the outer shape of the pig's body and the outlines of internal organs such as the heart. Current density vectors are plotted for one plane (though they are measured throughout the 3D volume) as blue coloured arrows. Streamlines are shown as red coloured curves. The outline of the heart is shown in fig. 2(a) as a green dashed line. The same data as figs. 2(a) and 2(b) are shown again in figs. 3(a) and 3(b) for the left-side view.

For current magnitude, $|\mathbf{J}|$, cumulative distribution curves were developed from histograms of data within the heart. Fig. 4 shows these cumulative distribution plots for the two experiments in all three states of VF, PM1 and PM2. The red coloured plot shows the AA data while the blue coloured dash-dot plot shows the AP data. The third curve, a blue coloured dashed line shows the AP data multiplied by a scale factor such that the $10^{th}$ percentile of the AA and AP distributions are matched. This matching of the $10^{th}$ percentile is done so that the shapes of the curves can be compared directly.

Table I gives the values of current flux in mA computed through the heart for VF, PM1 and PM2 experiments (Table I: column "Flux (mA)"). The current flux through the heart is divided by the total applied current to compute the percentage of current that reaches the heart for each experiment (Table I: column "% thru Heart"). In Table I, the column titled "% Change in Flux" shows the percent difference in current flux results between AA and AP measurements for each experiment. The final column in

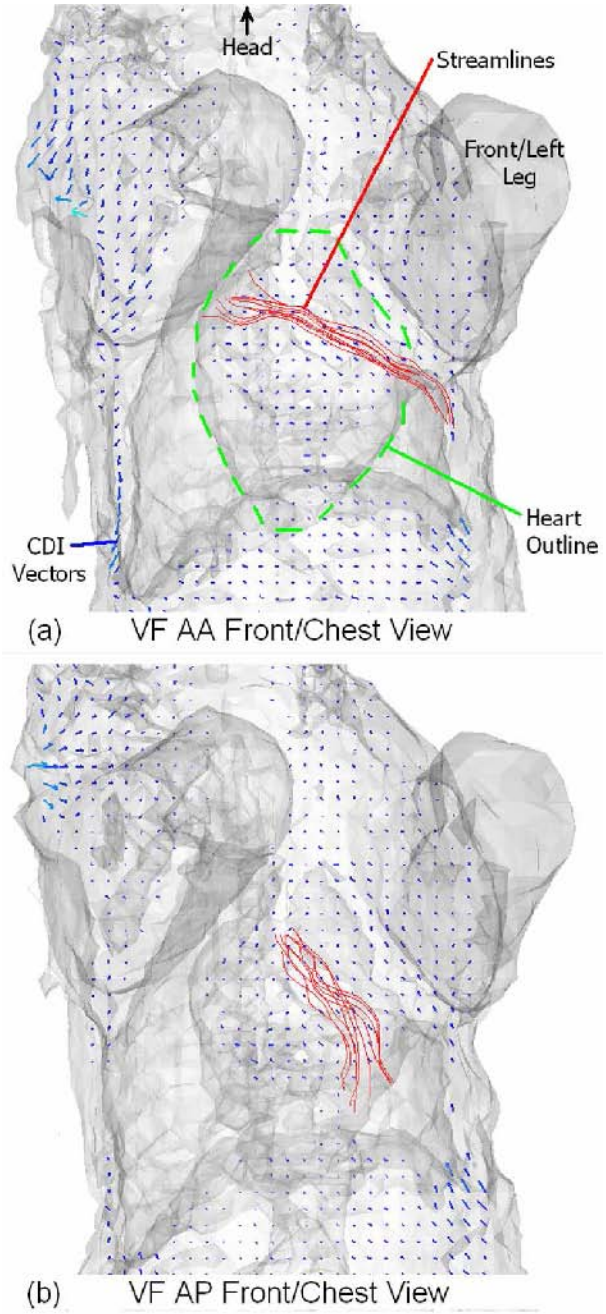


Fig. 2. (a) AA and (b) AP electrode positions showing the transparent anatomical MRI iso-surface data in gray colour, the vector plots as blue coloured arrows and the streamlines as red coloured curves. The outline of the heart is shown in (a) with a dashed green line.

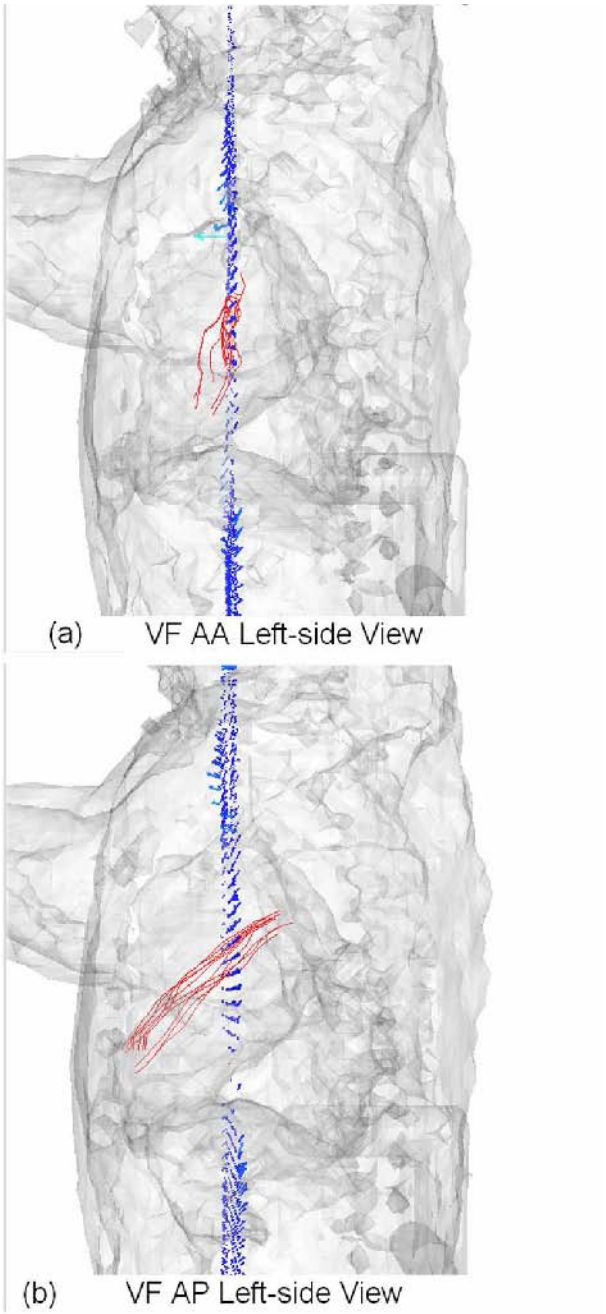


Fig. 3. (a) AA and (b) AP electrode positions showing the same data as in fig. 2 from the left-side view.

Table I, titled "% Change in $|\mathbf{J}|$", shows the percent difference in average current density magnitude for the heart between the AA and AP measurements for each experiment.

Fig. 5(b) shows a conductivity image computed from the integral of equation (3) for the heart. Fig 5(a) shows the MRI data corresponding to fig. 5(b).

## IV. Discussion

The comparison of AA and AP electrode positions demonstrates that the direction of current flow is highly dependent on electrode positioning. For the AA electrode position, the dominant direction of current flow appears to be across the torso (see fig. 2(a)) whereas for the AP position, the dominant direction appears to be from the apex of the heart towards the back (see fig. 3(b)).

The cumulative distribution plots of $|\mathbf{J}|$ show that more current is delivered to the heart with the AP electrode positions than with AA because the AP curve is located further to the right than the AA curve. The slopes of the curves, which indicate distribution of $|\mathbf{J}|$ values, appear to be similar for both AA and AP for one given experiment. There is greater variance in $|\mathbf{J}|$ distribution observed from one

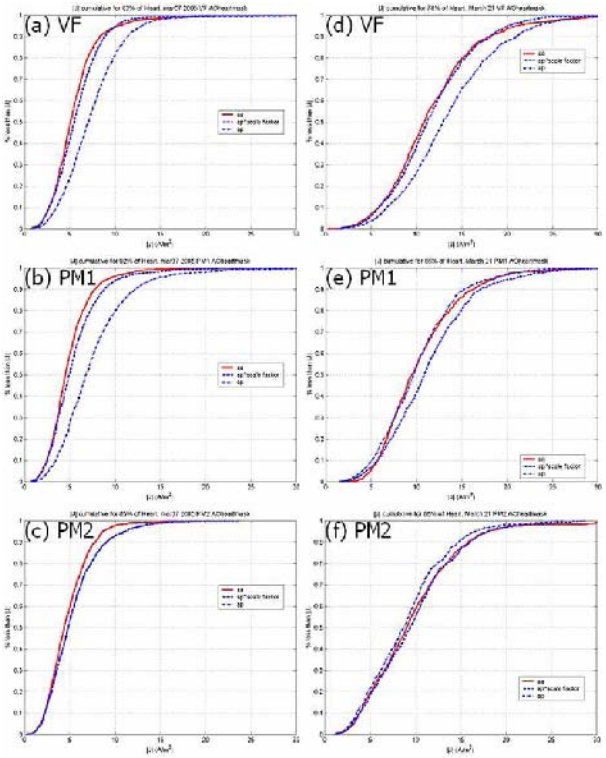


Fig. 4. Cumulative distribution plots for $|\mathbf{J}|$ for (a), (b), (c) 4.0 kg pig #1 and (d), (e), (f) 4.6 kg pig #2. AA curve is red solid and AP curve is blue dash-dot. Blue dash curve is AP curve scaled such that 10$^{th}$ percentiles are matched between AA and AP.

animal to another. The amount of current reaching the heart is substantially different between AA and AP during VF, but this difference fades away as post-mortem time progresses.

The results shown in Table I quantitatively demonstrate that there is 15 to 32% more current delivered to the heart for AP electrode positioning than for AA. These results also demonstrate that these differences fade away as post-mortem time progresses (the notable exception being PM1 for experiment #1).

The conductivity image in fig. 5 shows higher conductivity for blood in the right ventricle compared with blood in the left ventricle. Perhaps the blood is substantially ejected from the left ventricle. Conductivity of the myocardium generally appears less than that of the blood as expected; however, conductivity computations for myocardium are unreliable due to the assumption of isotropy

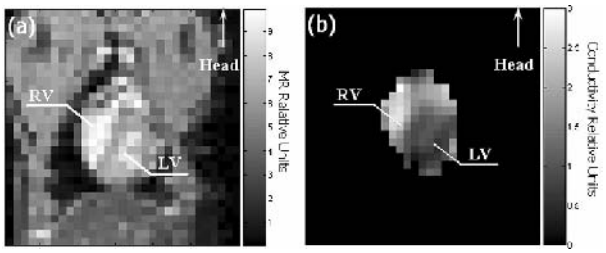


Fig. 5. (a) MRI anatomical data showing a coronal slice through ventricles and (b) corresponding conductivity image for experiment #2, i.e. 140 mA. Right ventricle, denoted RV, and left ventricle, denoted LV, are shown with relative conductivity substantially higher in RV.

TABLE I
COMPARISON OF CURRENT FLUX AND $|\mathbf{J}|$ FOR AA AND AP

| Exp. | State | Cfg. | Flux (mA) | % thru Heart | % Change in Flux | % Change in $\|\mathbf{J}\|$ |
|---|---|---|---|---|---|---|
| #1 58 mA | VF | AA | 10.4 | 17.9 | 32.6 *** | 28.7 *** |
| | | AP | 14.5 | 24.9 | | |
| | PM1 | AA | 8.8 | 15.2 | 40.1 *** | 40.9 *** |
| | | AP | 13.2 | 22.8 | | |
| | PM2 | AA | 8.1 | 13.9 | 17.4 *** | 10.9 *** |
| | | AP | 9.6 | 16.5 | | |
| #2 140 mA | VF | AA | 20.8 | 14.8 | 16.5 *** | 15.0 *** |
| | | AP | 24.5 | 17.5 | | |
| | PM1 | AA | 17.3 | 12.4 | 8.6 *** | -2.5 *** |
| | | AP | 18.9 | 13.5 | | |
| | PM2 | AA | 14.8 | 10.5 | -3.3 ** | -7.8 *** |
| | | AP | 14.3 | 10.2 | | |

*** % difference is greater than 3 times standard error
** % difference is greater than 2 time standard error.

which is known to be a poor assumption for the myocardium [9]. The fact that conductivity can be computed from current density vector data implies the possibility of computing voltage potentials. Voltage computations were not performed as part of this work at this time.

## V. CONCLUSION

The 3D FGRE CDI sequence is a research tool that offers measurements of many electrical properties of biological tissue. This work verifies that more electricity reaches the myocardium for AP electrode positioning than for AA.

## ACKNOWLEDGMENT

T. P. DeMonte, would like to thank Charles Yan, Ning Zhang and Tom Lyster for their contributions to this work.

## REFERENCES

[1] G. C. Scott, M. L. G. Joy, R. L. Armstrong, R. M. Henkelman. Measurement of nonuniform current density by magnetic resonance. *IEEE Trans. Med. Imag,,* Vol. 10, No. 3, pp. 362-374, 1991.

[2] T. P. DeMonte, R. S. Yoon, D. B. Jorgenson, and M. L. G. Joy, "A System for In-Vivo Cardiac Defibrillation Current Density Imaging in a Pig," in *Proc. 25th Annu IEEE Int. Conf. EMBS*, Cancun, 2003.

[3] S. Marinkovic et al, *Sectional and MRI anatomy of the human body: a photographic atlas*, Thieme, 2000.

[4] T. O. Odlaug, *Laboratory anatomy of the fetal pig*. W. C. Brown Co., 1980.

[5] R. S. Yoon, T. P. DeMonte, K. F. Hasanov, D. B. Jorgenson, and M. L. G. Joy, "Vector Analysis of Current Pathways in Post-mortem Pig Torso," in *Proc. 10th Annu. ISMRM Int. Conf*., Hawaii, 2002.

[6] Rachel Chan Undergraduate Thesis, University of Toronto, 2005.

[7] I. Sobel. "An isotropic 3 x 3 image gradient operator," in *Machine Vision for Three-Dimensional Scenes*, H. Freeman, Ed. Academic Press, 1990, pp. 376-379.

[8] M. L. Joy, A. I. Nachman, K. F. Hasanov, R. S. Yoon and, A. W. Ma, "A new approach to Current Density Impedance Imaging (CDII)," in *Proc. 12th Annu. ISMRM Int. Conf*., Kyoto, Japan, 2004.

[9] Y. Wang, D. R. Haynor, and Y. Kim, An investigation of the importance of myocardial anisotropy in finite-element modeling of the heart: methodology and application to the estimation of defibrillation efficacy. *IEEE Trans. Biomed. Eng*., vol. 48, pp. 1377-1389, Dec 2001.